

Precision measurements on δ_{CP} in MOMENT

Jian Tang, Sampsa Vihonen, Tse-Chun Wang

School of Physics, Sun Yat-Sen University,

No. 135, Xingang Xi Road, Guangzhou, 510275, P. R. China

E-mail: tangjian5@mail.sysu.edu.cn, sampsa@mail.sysu.edu.cn,
wangzejun@mail.sysu.edu.cn

ABSTRACT: As it is very promising to expect a discovery of CP violation in the leptonic sector, the precision measurement of the Dirac CP phase δ_{CP} is going to be one of the key interests in the future neutrino oscillation experiments. In this work, we examine the physics reach of the proposed medium baseline muon decay experiment MOMENT. In order to identify potential bottlenecks and opportunities to improve CP precision in MOMENT, we investigate the effect of statistical error, systematic uncertainties, fraction of the muon beam polarity, and adjusting the baseline length to match the first or second oscillation maximum on the precision measurement of δ_{CP} . We also simulate superbeam experiments T2K, NO ν A, T2HK, DUNE and T2HKK in comparison and complementary to MOMENT. To reach the precision of δ_{CP} at 12° or better at 1σ confidence level, we find it sufficient to combine the data of MOMENT, DUNE and T2HK.

Contents

1	Introduction	1
2	A brief review of the oscillation probabilities in CP precision	3
3	Simulation details	5
4	Precision measurement of δ_{CP} in MOMENT	8
4.1	Sensitivity to the δ_{CP} parameter in MOMENT	9
4.2	Optimizing the δ_{CP} measurement in MOMENT	10
4.2.1	Statistical uncertainties	10
4.2.2	Systematic uncertainties	11
4.2.3	Beam polarity	12
4.2.4	First and second oscillation maxima	13
4.3	Complementarity of MOMENT and superbeam experiments in the measurement of δ_{CP}	14
5	Summary	16
6	Appendix	18
A	The long baseline neutrino experiments considered in this work	18
A.1	T2K	18
A.2	NO ν A	18
A.3	T2HK and T2HKK	19
A.4	DUNE	19
B	The effects of detector efficiencies and atmospheric neutrino background on the results	20

1 Introduction

Neutrino physics has experienced a steady flow of progress since the confirmation of neutrino oscillations was made in Super-Kamiokande and Sudbury Neutrino Observatory nearly two decades ago [1, 2]. This has been achieved in the many reactor, solar, atmospheric and accelerator neutrino experiments that have operated since then.

The oscillation of three neutrinos can be parametrized in terms of six physical variables [3–5]: the three mixing angles θ_{12} , θ_{13} and θ_{23} , the two mass-squared differences $\Delta m_{21}^2 = m_2^2 - m_1^2$ and $\Delta m_{31}^2 = m_3^2 - m_1^2$, and the Dirac CP phase δ_{CP} . These parameters have been measured to a high precision (see Refs. [6–9] for reviews). Whereas the best-fit

values of the so called solar parameters θ_{12} and Δm_{21}^2 have been determined with the relative precisions of 14% and 16% at 3σ confidence level (CL), respectively, the precision of the so called reactor mixing angle θ_{13} is 8.9% [6]. The value of the atmospheric mixing angle θ_{23} is less precisely known, with 23% at 3σ , and it is not well known whether it resides in the high octant $\theta_{23} > 45^\circ$, or the low octant, $\theta_{23} < 45^\circ$. The sign of the atmospheric mass splitting $\Delta m_{3\ell}^2$, where $\ell = 1$ for the normal ordering ($m_1 < m_2 \ll m_3$) and 2 for inverted ordering ($m_3 \ll m_1 < m_2$), is currently unknown, but its magnitude $|\Delta m_{3\ell}^2|$ has been measured with the relative precision of 7.5%. Most recently, a global fit from the neutrino oscillation data has provided a best-fit for the Dirac CP phase at $\delta_{\text{CP}} \simeq 221^\circ$, when the mass ordering is normal, and $\delta_{\text{CP}} \simeq 282^\circ$ when the ordering is inverted [6]. The signal remains statistically insignificant, however, and the values of $\delta_{\text{CP}} = 144\dots357^\circ$ are still available within the 3σ CL bounds.

Precision measurements on the neutrino oscillation parameters open up an opportunity to search for the origin of neutrino mixing, e.g. a flavour symmetry [10]. One of the key parameters in discriminating between the various available flavour symmetries is the Dirac CP phase δ_{CP} , which is desirable to be known by approximately 10° uncertainty at 1σ CL in the event where the value δ_{CP} is confirmed to lie near 270° (see e.g. Ref. [11]). The precision measurements of δ_{CP} in future experiments have been previously discussed in e.g. Refs. [12–16].

Future neutrino oscillation experiments will play an important role in curtailing the error on δ_{CP} . In this work, we investigate the precision measurement of δ_{CP} in the MuOn-decay MEdium baseline NeuTrino beam facility (MOMENT) [17]. MOMENT is proposed to use a novel approach to generate a very intensive beam of neutrinos and antineutrinos via the decay of positive and negative muons, which allows to survey neutrino oscillations in eight different channels. In the past, MOMENT and its physics potential have been studied in CP violation discovery [18, 19], non-standard neutrino interactions [19, 20] and invisible neutrino decays [21].

In the present work, we study the physics potential of MOMENT in the standard three neutrino oscillations and compare its sensitivities with those of the currently running long baseline neutrino experiments T2K [22] and NO ν A [23], as well as the next generation experiments T2HK [24] and DUNE [25]. We also discuss the option of placing the second Hyper-Kamiokande detector in Korea, as was suggested in the T2HKK [26] proposal. We find that MOMENT has an excellent sensitivity for the precision measurement of δ_{CP} at its current best-fit values. We also find that MOMENT can measure δ_{CP} by 15° uncertainty or better at 1σ CL for approximately 76% of its currently allowed values.

This paper is organized as follows: In Section 2, we review the oscillation probabilities relevant for MOMENT and discuss the role of the first and second oscillation maxima in the precision measurement of δ_{CP} . In Section 3, we give a brief introduction to the experimental setup of MOMENT and describe how its simulation is done in this work. We present the results of this work in Section 4, and summarize our findings in Section 5.

2 A brief review of the oscillation probabilities in CP precision

In this section, we perform an analytical study on the neutrino oscillation probabilities that are relevant for δ_{CP} precision in the experiments considered in this work.

The precision on the δ_{CP} parameter can be extracted in neutrino oscillation experiments by comparing the spectral data from the neutrino and antineutrino oscillation channels. In conventional beam experiments such as T2K and NO ν A, the sensitivity to the δ_{CP} parameter is mainly facilitated by comparing the measured event and energy spectra in the appearance channels $\nu_\mu \rightarrow \nu_e$ and $\bar{\nu}_\mu \rightarrow \bar{\nu}_e$, from which the value of δ_{CP} can then be resolved.

Neutrino experiments based on muon decay are different from superbeams by the number of oscillation channels which can be used for the determination of the δ_{CP} value. MOMENT, for example, benefits from the simultaneous access to the channels $\nu_e \rightarrow \nu_\mu$ and $\bar{\nu}_\mu \rightarrow \bar{\nu}_e$ when the experiment runs in the μ^+ beam mode, and to their conjugate channels $\bar{\nu}_e \rightarrow \bar{\nu}_\mu$ and $\nu_\mu \rightarrow \nu_e$ when it is in the μ^- mode. When the corresponding disappearance channels are taken into account, the experiment gains access to eight channels in total.

Let us begin by considering the oscillations of the neutrinos that originate from the μ^+ beam. The probabilities for the appearance channels $\nu_e \rightarrow \nu_\mu$ and $\bar{\nu}_\mu \rightarrow \bar{\nu}_e$ can be approximated with the following analytical expressions [12, 14, 27]. Taking the quantity $\varepsilon \equiv \Delta m_{21}^2/\Delta m_{31}^2$ to be small, such that $\sin^2 \theta_{13} \sim \mathcal{O}(\varepsilon)$, the appearance probabilities can be expressed in powers of ε . For example, in the case of $\nu_e \rightarrow \nu_\mu$ channel, one gets

$$P_{\nu_e \rightarrow \nu_\mu} = P_1 + P_{3/2} + \mathcal{O}(\varepsilon^2). \quad (2.1)$$

Whereas the first-order term P_1 is independent of δ_{CP} ,

$$P_1 = \frac{4}{(1-r_A)^2} \sin^2 \theta_{23} \sin^2 \theta_{13} \sin^2 \left(\frac{(1-r_A)\Delta L}{2} \right), \quad (2.2)$$

the other term depends on the value of the δ_{CP} parameter:

$$P_{3/2} = 8 J_r \frac{\varepsilon}{r_A(1-r_A)} \cos \left(\delta_{\text{CP}} - \frac{\Delta L}{2} \right) \sin \left(\frac{r_A \Delta L}{2} \right) \sin \left(\frac{(1-r_A)\Delta L}{2} \right). \quad (2.3)$$

In the above expressions $J_r = \cos \theta_{12} \sin \theta_{12} \cos \theta_{23} \sin \theta_{23} \sin \theta_{13}$ is the reduced Jarlskog invariant, L is the baseline length and E is the energy of the neutrino or antineutrino. The matter effects enter the probability via $r_A = \sqrt{2} G_F N_e / \Delta$, where N_e is the electron number density, G_F the Fermi coupling constant and $\Delta \equiv \Delta m_{31}^2 / 2E$.

As is apparent in Eqs. (2.1–2.3), the sensitivity to δ_{CP} arises from the $P_{3/2}$ term, which is dependent on the value of δ_{CP} through $\cos(\delta_{\text{CP}} - \Delta L/2)$. The maximum value of $P_{3/2}$ is therefore attained when $\Delta L/2 \simeq (2n+1)\pi/2$, $n = 0, 1, 2, \dots$, and the minimum when $\Delta L/2 \simeq n\pi$, respectively. The first oscillation maximum is said to occur when $\Delta L/2 \simeq \pi/2$, and the second oscillation maximum when $\Delta L/2 \simeq 3\pi/2$. When the condition for either oscillation maximum is met, the dependence on δ_{CP} can be approximated as $P_{3/2} \propto \sin \delta_{\text{CP}}$.

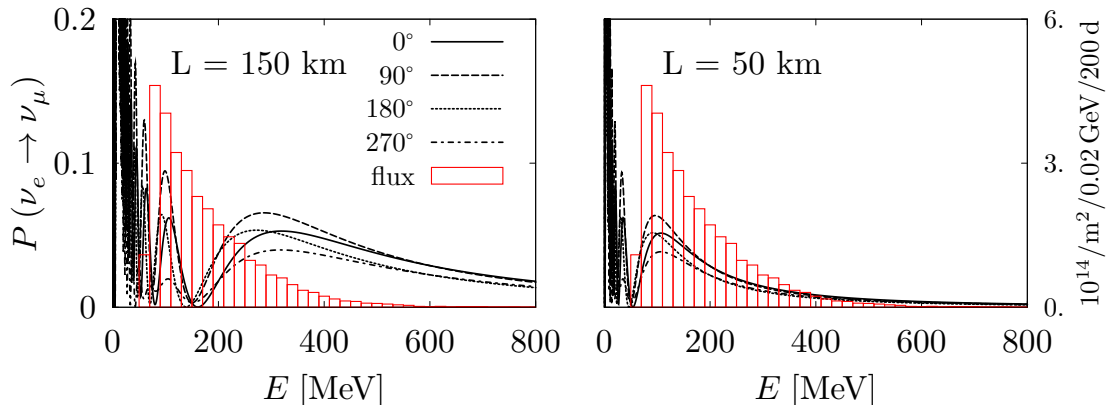


Figure 1: The transition probability for the $\nu_e \rightarrow \nu_\mu$ channel, presented for the values $\delta_{\text{CP}} = 0^\circ, 90^\circ, 180^\circ$ and 270° . The probabilities are shown as functions of the neutrino energy $E = 0 \dots 800$ MeV. In the left panel, the probabilities are shown for the experimental configuration where the baseline length L is optimized for the second oscillation maximum ($L = 150$ km). In the right panel, the probabilities are correspondingly shown for the first oscillation maximum ($L = 50$ km). For convenience, the simulated electron neutrino fluxes for MOMENT are shown with the red boxes. The fluxes are given in units of $10^{14}/\text{m}^2/0.02 \text{ GeV}/200 \text{ d}$.

The other probability relevant to the μ^+ beam, $P_{\bar{\nu}_\mu \rightarrow \bar{\nu}_e}$, can be conveniently obtained from Eqs. (2.1-2.3) via the transformation $r_A \rightarrow -r_A$. Knowing that the matter potentials are small in medium-baseline experiments like MOMENT, we remark that $P_{\nu_e \rightarrow \nu_\mu}$ and $P_{\bar{\nu}_\mu \rightarrow \bar{\nu}_e}$ take approximately the same size and shape.

When the oscillations originating from the μ^- beam are concerned, the relevant oscillation channels for δ_{CP} measurements are $\nu_\mu \rightarrow \nu_e$ and $\bar{\nu}_e \rightarrow \bar{\nu}_\mu$. The expression for the $\nu_\mu \rightarrow \nu_e$ probability can be acquired from Eqs. (2.1-2.3) through the transformation $\delta_{\text{CP}} \rightarrow -\delta_{\text{CP}}$. The probability for $\bar{\nu}_e \rightarrow \bar{\nu}_\mu$ can be similarly obtained via the transformations $\delta_{\text{CP}} \rightarrow -\delta_{\text{CP}}$ and $r_A \rightarrow -r_A$, leading to similar behaviour near the oscillation maxima.

One can make an estimate on the size of the relative uncertainty that is attainable on the true value of δ_{CP} in a neutrino oscillation experiment [12, 14]. Owing to the sinusoidal nature of the $\sin \delta_{\text{CP}}$ term in $P_{3/2}$, one can expect the best resolution to the individual values of δ_{CP} near the CP conserving values $\delta_{\text{CP}} = 0, \pi$ and the worst resolution near $\delta_{\text{CP}} = \pi/2, 3\pi/2$, respectively. When the oscillations take place in vacuum ($r_A = 0$) the correspondence is exact, whereas the presence of matter effects shifts the maximal and minimal sensitivities away from their respective values in vacuum. In such a case, the direction of the shift corresponds to the sign of Δm_{31}^2 , as well as to the CP phase of the neutrino/antineutrino beam.

In this work, we focus on analysing the physics reach of MOMENT. The simulation of MOMENT is done with the General Long-Baseline Simulator (GLOBES) library [28, 29] following the simulation details that were defined in Ref. [20]. The relevant oscillation

probabilities for MOMENT are presented in Fig. 1, where the oscillation probabilities corresponding to $\bar{\nu}_\mu \rightarrow \bar{\nu}_e$ and $\nu_e \rightarrow \nu_\mu$ transitions are plotted for the true values $\delta_{\text{CP}} = 0^\circ, 90^\circ, 180^\circ$ and 270° with solid, dashed, dotted and dot-dashed lines, respectively. The electron neutrino fluxes used in our simulation of MOMENT are illustrated with the solid red lines. The fluxes are given in units of $\nu/\text{m}^2/0.02 \text{ GeV}/200 \text{ d}$ and defined at the source.

As is apparent from Fig. 1, the neutrino fluxes used in our simulation of MOMENT can be sensitive to either the first or second oscillation maximum. The electron neutrino fluxes shown in the figure peak at $E \simeq 100 \text{ MeV}$, corresponding to the second oscillation maximum at the default baseline of $L = 150 \text{ km}$. In principle, the experimental setup could be optimized for the first oscillation maximum by moving the detector closer to the beam facility, such that $L = 50 \text{ km}$. This configuration could alternatively be sought by configuring the neutrino beam to peak at the energies $E \simeq 300 \text{ MeV}$.

Fig. 1 illustrates the effect of varying the δ_{CP} parameter in the appearance probability $P(\nu_e \rightarrow \nu_\mu)$. In the left panel of the figure, the probability for $\delta_{\text{CP}} = 0^\circ$ is nearly three times larger than the probability for $\delta_{\text{CP}} = 270^\circ$, when neutrino energies near the second oscillation maximum are considered. In the right panel, on the other hand, the variation near the first oscillation maximum is less significant, though the wider shape of the oscillation maximum can be expected to yield a greater number of events.

3 Simulation details

In this section we describe the experimental setup of MOMENT that is assumed for the simulations. The schematic design of the beam facility is presented in Ref. [17].

MOMENT entails a novel idea of producing a very intense neutrino-antineutrino beam at relatively low energies. In the plan, MOMENT includes a 1.5 GeV proton linac and a 10 mA proton driver, and it is aimed to produce a 15 MW proton beam in a continuous wave. The proton beam is proposed to hit a mercury jet-target, creating a beam of charged mesons mostly consisting of pions and kaons. The number of protons expected to hit the jet-target is 1.1×10^{24} per year. Super-conducting solenoids are then used to select pions of the desired energy range to be led to a decay tunnel. The selected pions decay in the tunnel into positively and negatively charged muons, which are further led to a 600 m decay tunnel where they can decay into neutrinos and antineutrinos. Whereas the positively charged muons decay into positrons and $\nu_e \bar{\nu}_\mu$ pairs, the negatively charged muons decay into electrons and $\bar{\nu}_e \nu_\mu$ pairs. The resulting beam of neutrinos and antineutrinos is expected to peak roughly at 200 MeV energy.

In the original proposal [17], the beam facility is proposed to be placed at the China Spallation Neutron Source whereas the location of the far detector is suggested to be near the JUNO far detector site, constituting a baseline of 150 km length. A far detector of approximately 500 kton mass has been suggested for this purpose. In previous works (see e.g. Ref. [20]), a Water Čerenkov detector with Gd-doping has been considered due to its excellent performance at low energies.

MOMENT benefits from well-constrained backgrounds from the source thanks to its muon-decay-based production mechanism. The main sources of background in MOMENT

Table 1: The experimental inputs assumed in the simulation of MOMENT and the long baseline experiments T2K, NO ν A, DUNE, T2HK and T2HKK. The energy resolution is given in terms of σ_e , which corresponds to the width of the Gaussian distribution.

Experiment	T2K	NO ν A	DUNE	T2HK	MOMENT	T2HKK
Location	Japan	USA	USA	Japan	China	Japan
Status	operating	operating	under construction	proposed	proposed	proposed
Accelerator facility	J-PARC	Fermilab	Fermilab	J-PARC	MOMENT	J-PARC
Beam power	770 kW	700 kW	1.07 MW	1.3 MW	15 MW	1.3 MW
Expected POT	7.8×10^{21}	3.6×10^{21}	1.47×10^{21}	1.56×10^{22}	1.1×10^{25}	1.56×10^{22}
Baseline length	295 km	810 km	1300 km	295 km	150 km	295 km & 1100 km
Off-axis angle	2.5°	0.8°	0°	2.5°	0°	2.5° & 1.5°
Detector technology	W.C.	L.Sc.	L.Ar.	W.C. & W.C.	W.C.	W.C. & W.C.
Fiducial mass	22.5 kt	14 kt	40 kt	187 kt & 187 kt	500 kt	187 kt & 187 kt
Running times (years)	2+6	3+3	5+5	2.5+7.5	5+5	2.5+7.5
Energy window (GeV)	[0.4, 1.2]	[1.0, 3.5]	[0.5, 18.0]	[0.1, 10.0]	[0.1, 0.8]	[0.1, 10.0]
Energy bins	20	25	71	12	20	12
$\sigma_e = \alpha E + \beta \sqrt{E} + \gamma$	$\gamma = 0.085$ GeV	$\beta = 10\%$ (e-like) $\beta = 5\%$ (μ -like)	migration matrices	migration matrices	$\alpha = 8.5\%$	migration matrices
References	Ref. [22]	Ref. [23]	Ref. [25]	Ref. [24]	Ref. [17]	Ref. [26]

are charge mis-identification, detector imperfections, atmospheric neutrinos and neutral current backgrounds [18, 20]. All of these background components set limitations to the experiments physics reach, and thus require a careful study.

In this work, we simulate a 10-year-long run in MOMENT, shared evenly between the μ^+ run and the μ^- run. The simulation details concerning the 500-kton Water Čerenkov detector with Gd-doping as well as the beam facility are summarized in Table 1. The information of the detector design follows the description given in Ref. [30], Gd-doping technology in Ref. [31], and atmospheric neutrino background suppression in Refs. [32] and [33]. The neutrino and antineutrino fluxes are based on a Monte Carlo simulation provided by the accelerator working group [20], assuming 1.1×10^{24} POT per year (corresponding to 3.8×10^{21} neutrinos per year). The cross sections for the charged current and neutral current processes are taken from Ref. [34], respectively. In order to make a comparison or a combination of different experiments, we also include the simulations of T2K and NO ν A as well as of DUNE, T2HK and T2HKK. We take the simulation files for T2K [35–37] and NO ν A [38, 39] from the GLOBES website [40], whilst the files for DUNE are obtained from Ref. [41] and those of T2HK and T2HKK from the respective collaboration. The details of each long baseline experiment are summarized in Table 1 and Appendix A.

Regarding the simulation of the 500 kt Gd-doped WC detector, we adopt the same methodology as what was used in Ref. [20]. Throughout our work, we assume a 40% reconstruction efficiency for electron-like events and 50% efficiency for muon-like events, respectively. As far as the background is concerned, we assign a 0.3% acceptance rate for wrong-charge particles being tagged as signal events and 0.25% rate for events originating from neutral current interactions.

Table 2: The current best-fit values and 1σ uncertainties for the neutrino oscillation parameters [6]. These values are shown for both mass orderings and are taken from a recent global analysis. Note that Δm_{3l}^2 stands for Δm_{31}^2 in normal ordering (NO) and Δm_{32}^2 in inverted ordering (IO).

Parameter	Central value $\pm 1\sigma$ (NO)	Central value $\pm 1\sigma$ (IO)
θ_{12} ($^\circ$)	33.82 ± 0.78	33.82 ± 0.78
θ_{13} ($^\circ$)	8.60 ± 0.13	8.64 ± 0.13
θ_{23} ($^\circ$)	48.6 ± 1.4	48.8 ± 1.2
δ_{CP} ($^\circ$)	221 ± 39	282 ± 25
Δm_{21}^2 (10^{-5} eV 2)	7.39 ± 0.21	7.39 ± 0.21
Δm_{3l}^2 (10^{-3} eV 2)	2.528 ± 0.031	-2.510 ± 0.031

For the atmospheric neutrino background, we assume the same treatment as was done in Ref. [30]. We calculate the number of events from the atmospheric neutrino background in each energy bin as follows:

$$N_i = T N_{\text{nucl}} f \int_{E_{\text{min}}}^{E_{\text{max}}} dE \int_{E'_{\text{min}}}^{E'_{\text{max}}} dE' \phi(E) \sigma(E) R(E, E'), \quad (3.1)$$

where i is the number of energy bin, T is the total runtime of the experiment and N_{nucl} is the number of target nucleons in the detector. The true and reconstructed energies are denoted as E and E' , respectively. Whereas $E_{\text{min}} = 100$ MeV and $E_{\text{max}} = 800$ MeV are the boundaries of the considered energy range, E'_{min} and E'_{max} denote the boundaries of the energy bin. The atmospheric neutrino fluxes are given by $\phi(E)$, while $\sigma(E)$ stands for the cross sections and $R(E, E')$ is the energy resolution function. The atmospheric neutrino flux is constrained by the suppression factor f , which we take to be 2.2×10^{-3} after angular cuts and measuring the atmospheric background during the beam-off time.¹

From now on, we briefly describe how the χ^2 values are calculated and what parameter values are used in the simulation. The central values for the oscillation parameters are taken from the corresponding best-fit values, which are summarized in Table 2.

The statistical part of the χ^2 function is calculated with the well-known Poissonian [28]:

$$\chi^2(\vec{\omega}, \vec{\omega}_0, \zeta_{\text{sg}}, \zeta_{\text{bg}}) = \sum_{i=1}^{20} 2 \left[T_i - O_i \left(1 + \ln \frac{T_i}{O_i} \right) \right], \quad (3.2)$$

where $\vec{\omega} \equiv (\theta_{12}, \theta_{13}, \theta_{23}, \delta_{\text{CP}}, \Delta m_{21}^2, \Delta m_{31}^2)$ and $\vec{\omega}_0$ are the so called test and true values of the oscillation parameters, O_i and T_i are the event numbers corresponding to $\vec{\omega}$ and $\vec{\omega}_0$, and

¹In Refs. [18, 33], the suppression factor is given by Nl/L , where N is the number of ion or proton bunches, L is the length of the decay volume, while l gives the distance between two bunches. In both definitions, smaller suppression factors correspond to better reduction of the atmospheric neutrino background.

ζ_{sg} and ζ_{bg} are the nuisance parameters describing the overall normalization error for the signal and background events, respectively. O_i and T_i are obtained from $\vec{\omega}$ and $\vec{\omega}_0$ as follows: $O_i(\vec{\omega}_0) = N_i^{\text{sg}}(\vec{\omega}_0) + N_i^{\text{bg}}(\vec{\omega}_0)$ and $T_i(\vec{\omega}, \zeta_{\text{sg}}, \zeta_{\text{bg}}) = (1 + \zeta_{\text{sg}}) N_i^{\text{sg}}(\vec{\omega}) + (1 + \zeta_{\text{bg}}) N_i^{\text{bg}}(\vec{\omega})$, where N_i^{sg} and N_i^{bg} represent the expected numbers for signal and background events, respectively.

The χ^2 value corresponding to a neutrino signal, e.g. from events originating from $\nu_e \rightarrow \nu_\mu$ oscillation, is estimated from the Poissonian shown in Eq. (3.2) after including the systematics with the conventional pull method and applying the experimental uncertainties with the priors:

$$\chi^2(\vec{\omega}_0) = \min_{\vec{\omega}, \zeta_{\text{sg}}, \zeta_{\text{bg}}} \left[\chi_{\text{stat}}^2(\vec{\omega}, \vec{\omega}_0, \zeta_{\text{sg}}, \zeta_{\text{bg}}) + \frac{\zeta_{\text{sg}}^2}{\sigma_{\text{sg}}^2} + \frac{\zeta_{\text{bg}}^2}{\sigma_{\text{bg}}^2} + \sum_{k=1}^6 \left(\frac{\omega_k - (\omega_0)_k}{\sigma_k} \right)^2 \right], \quad (3.3)$$

where σ_{sg} and σ_{bg} are the errors associated with the nuisance parameters ζ_{sg} and ζ_{bg} , respectively. The minimization in Eq. (3.3) is first performed over the nuisance parameters ζ_{sg} and ζ_{bg} and then over the test values $\vec{\omega}$.

The overall χ^2 distributions are calculated by summing the χ^2 values corresponding to the relevant oscillation channels in the simulated experiment. Each channel is assigned with a signal and background error σ_{sg} and σ_{bg} , whereas the priors are taken from Table 2. In our simulation of MOMENT, we set $\sigma_{\text{sg}} = 0.025$ and $\sigma_{\text{bg}} = 0.05$ for electron-like events, and $\sigma_{\text{sg}} = 0.05$ and $\sigma_{\text{bg}} = 0.05$ for muon-like events.

The precision on the δ_{CP} parameter can be conveniently expressed with $\Delta\chi^2 = \chi^2 - \chi_{\text{min}}^2$, which is defined as the difference of χ^2 calculated at an arbitrary test value of δ_{CP} and at a value that is taken to be its true value. Throughout this work, we calculate $\Delta\chi^2$ by minimizing over all oscillation parameters except for δ_{CP} , and assuming the neutrino mass ordering and θ_{23} octant be known.

We express our results in terms of $\Delta\delta_{\text{CP}}$, which we define as the average of the higher and lower deviations from the expected central value, that is,

$$\Delta\delta_{\text{CP}} = \frac{\delta_{\text{CP}}^{\text{upper}} - \delta_{\text{CP}}^{\text{lower}}}{2}, \quad (3.4)$$

where $\delta_{\text{CP}}^{\text{upper}}$ and $\delta_{\text{CP}}^{\text{lower}}$ are the upper and lower bounds, respectively, that can be expected to be attainable in the simulated neutrino experiment. In this work, we focus on the 1σ confidence level, at which it is sufficient to approximate $\Delta\chi^2$ as a χ^2 distribution of one degree of freedom. Here $\delta_{\text{CP}}^{\text{upper}}$ and $\delta_{\text{CP}}^{\text{lower}}$ are determined as the fit values that satisfy the requirement $\Delta\chi^2 = 1$.

4 Precision measurement of δ_{CP} in MOMENT

We present the results of our work in this section. In Section 4.1, we show sensitivity to the Dirac CP phase δ_{CP} in MOMENT. We compare the sensitivities of MOMENT with those of currently running long baseline oscillation experiments T2K and NO ν A, and proposed next-generation experiments T2HK and DUNE. In Section 4.2, we investigate the impact of several experimental parameters on the δ_{CP} sensitivity in MOMENT. More specifically, we study the effects of statistics, systematics and beam polarity. We also discuss the effect

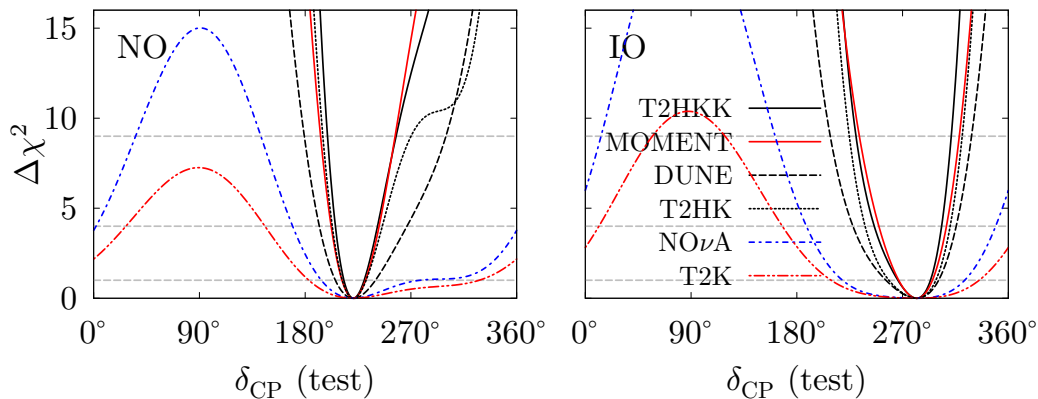


Figure 2: The sensitivity to the δ_{CP} parameter in neutrino oscillation experiments. The $\Delta\chi^2$ distributions of the δ_{CP} parameter are shown for its allowed values $\delta_{\text{CP}} = 0^\circ \dots 360^\circ$. The 1σ , 2σ and 3σ confidence levels are shown with the dashed lines corresponding to $\Delta\chi^2 = 1, 4$ and 9 , respectively. The sensitivities are shown for MOMENT, T2HKK, DUNE, $\text{NO}\nu\text{A}$ and T2K, and for both normal (NO) and inverted mass orderings (IO).

of the second oscillation maximum in the measurement of δ_{CP} . Finally, in Section 4.3, we study the complementarity of MOMENT and the long baseline neutrino experiments in the precision of δ_{CP} .

4.1 Sensitivity to the δ_{CP} parameter in MOMENT

The sensitivity to the δ_{CP} parameter measurement is illustrated in Fig. 2. The figure presents the values of $\Delta\chi^2$ as function of $\delta_{\text{CP}} = 0^\circ \dots 360^\circ$, which are inserted as test values in Eq. (3.3). The true value of δ_{CP} is taken to be $\delta_{\text{CP}} = 221^\circ$ when the normal ordering (NO, $m_1 < m_2 \ll m_3$) is assumed, and $\delta_{\text{CP}} = 282^\circ$ when the ordering is taken to be inverted¹ (IO, $m_3 \ll m_1 < m_2$). The $\Delta\chi^2$ distributions are shown for δ_{CP} in T2K, $\text{NO}\nu\text{A}$, T2HK, DUNE, MOMENT and T2HKK. The results for T2K and $\text{NO}\nu\text{A}$ as well as for the future experiments are prediction forecasts. For convenience, the 1σ , 2σ and 3σ confidence level contours are shown with the lines $\Delta\chi^2 = 1, 4$ and 9 , respectively.

Our results predict excellent sensitivities to the precision of the δ_{CP} parameter in MOMENT. As can be seen in Fig. 2, the sensitivities of MOMENT can be expected to be comparable with those of future long baseline experiments DUNE and T2HK, as well as the T2HKK alternative, and superior to those of currently running long baseline experiments $\text{NO}\nu\text{A}$ and T2K.

¹The values of $\delta_{\text{CP}} = 221^\circ$ (NO) and $\delta_{\text{CP}} = 282^\circ$ (IO) correspond to the current best-fit values from fitting to the global neutrino oscillation data. The fits include the atmospheric neutrino data from Super-Kamiokande [6, 7].

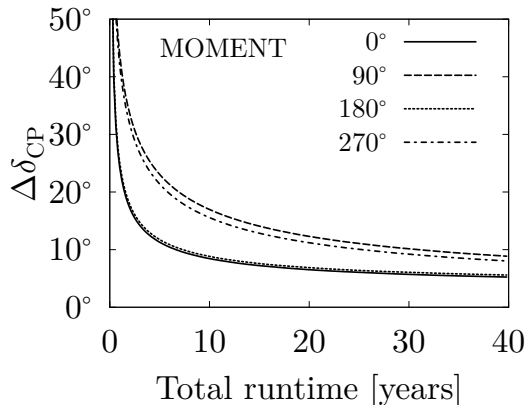


Figure 3: The effect of statistics on the precision measurement of δ_{CP} . The 1σ confidence level uncertainties for δ_{CP} are shown as a function of the total running time of the experiment. The $\Delta\delta_{\text{CP}}$ distributions are shown for the true values $\delta_{\text{CP}} = 0, 90^\circ, 180^\circ$ and 270° . The results are independent of the mass ordering.

4.2 Optimizing the δ_{CP} measurement in MOMENT

Though the physics reach of MOMENT has been studied in a number of references [18–21], it should be stressed that the experimental setup of MOMENT is still open. In this section we investigate the relevance of four different characteristics related to the experimental setup in the precision measurement of the δ_{CP} parameter. More specifically, we study how statistics, systematics, beam sharing and baseline length affect $\Delta\delta_{\text{CP}}$ in MOMENT. We also investigate how much the results depend on the assumptions that were made on the systematic uncertainties, detector efficiencies and the size of the background.

4.2.1 Statistical uncertainties

We first want to understand the relevance of statistics on the determination of $\Delta\delta_{\text{CP}}$ in MOMENT. We investigate this by studying the dependence of $\Delta\delta_{\text{CP}}$ on the running time of the experiment. In Fig. 3, $\Delta\delta_{\text{CP}}$ is shown as function of the total running time of the experiment, shared evenly between the μ^+ and μ^- modes. Since $\Delta\delta_{\text{CP}}$ also depends on the true value of δ_{CP} , we present the $\Delta\delta_{\text{CP}}$ contours for $\delta_{\text{CP}} = 0^\circ, 90^\circ, 180^\circ$ and 270° . We remark that NO and IO yield nearly identical numerical results.

Fig. 3 shows how increasing the total running time of the experiment, where the muon beam is shared evenly between the μ^+ and μ^- modes, leads to an improved result on $\Delta\delta_{\text{CP}}$. For the CP conserving values $\delta_{\text{CP}} = 0^\circ$ or 180° , the sensitivity becomes rather difficult to improve after 10 years of running. For example, doubling the running time from 10 years to 20 years improves the estimate on $\Delta\delta_{\text{CP}}$ by less than 2° . Increasing the running time further after 20 years leads to smaller improvements. For the maximally CP violating values $\delta_{\text{CP}} = 90^\circ$ and 270° , on the other hand, similar increases in running time leads to more significant improvements. All results are obtained at 1σ CL.

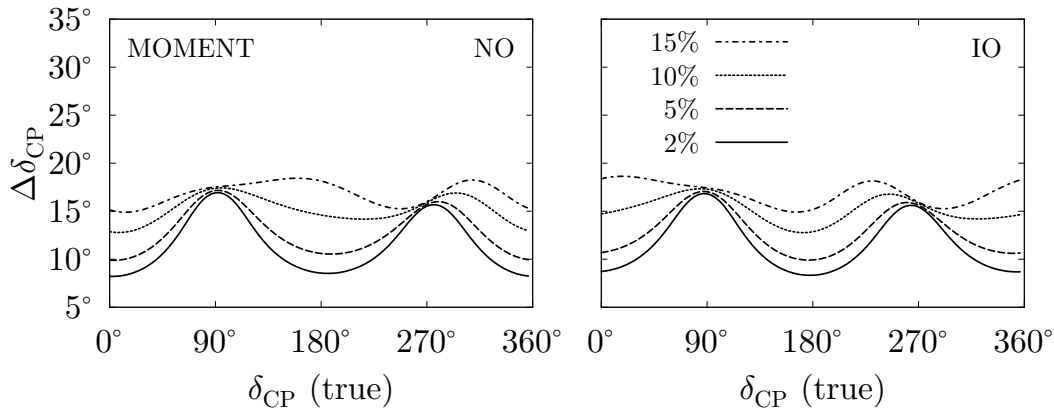


Figure 4: The effect of the systematics on the precision measurement of δ_{CP} . The 1σ confidence level uncertainties for δ_{CP} are shown as a function of values $\delta_{\text{CP}} = 0^\circ \dots 360^\circ$. The uncertainties are shown for four different scenarios where the systematic error on the signal normalization is set to either $\sigma_{\zeta_{\text{sg}}} = 2\%$, 5% , 10% or 15% . The results are shown for both normal (NO) and inverted ordering (IO).

One should keep in mind that increasing the running time is but one method to increase the statistics of the experiment. In principle, doubling the total running time is equivalent to doubling the fiducial mass of the detector or the intensity of the neutrino beam.

4.2.2 Systematic uncertainties

We next want to study the impact of the systematics on the precision of δ_{CP} in MOMENT. The importance of systematics is illustrated in Fig. 4, where $\Delta\delta_{\text{CP}}$ is plotted at 1σ CL as a function of δ_{CP} . The results are presented for four different values of $\sigma_{\zeta_{\text{sg}}}$, which we choose to be 2% , 5% , 10% and 15% . These errors correspond to the systematics arising from the overall normalization of the signal events, and it is set for relevant oscillation channels considered in this work. We assume a uniform signal normalization error in all signal events.

As is apparent from Fig. 4, the estimate on $\Delta\delta_{\text{CP}}$ at 1σ CL correlates with the considered systematics significantly for all values except the maximally CP violating values $\delta_{\text{CP}} = 90^\circ$ and 270° . This behaviour can be tracked back to the origin of CP sensitivity in $\sin\delta_{\text{CP}}$ (see Section 2). Hence, one may say that whilst δ_{CP} precision is dominated by systematics near the CP conserving values 0° and 180° , any improvements on the precision must be obtained through the increase of statistics near maximally CP violating values 90° and 270° , respectively.

We note that the simulation setup we defined for MOMENT in Section 3 leads to a sensitivity that is very similar to the 2% curve in Fig. 4. The default setup assumes a 2.5% systematic error on all appearance channels and 5% error on disappearance channels. The overlapping with the 2% error curve therefore highlights the importance of the appearance channels in the precision measurement on δ_{CP} .

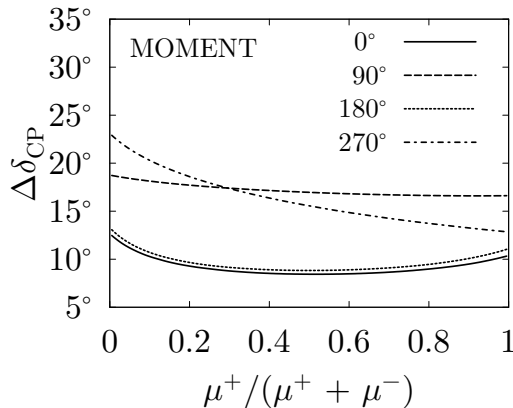


Figure 5: The effect of beam polarity on the precision measurement of δ_{CP} . The 1σ confidence level uncertainties for δ_{CP} are shown as a function of the fraction at which MOMENT operates in μ^+ mode, whereas the rest of the operation is run in μ^- mode. The uncertainties are shown for $\delta_{\text{CP}} = 0^\circ, 90^\circ, 180^\circ$ and 270° . The results are independent of the mass ordering.

We investigated the dependence of the results on the assumptions made on the systematic uncertainties, detector efficiencies and size of the background. The results are presented in Appendix B. We find that any changes to the detector efficiencies or background shift the $\Delta\delta_{\text{CP}}$ distributions either to the better or the worse. The shift is the most significant for $\delta_{\text{CP}} = 90^\circ$ and 270° , and the least significant for $\delta_{\text{CP}} = 0^\circ$ and 180° , respectively.

4.2.3 Beam polarity

We next set our focus on the importance of the beam polarity in the precision of the δ_{CP} parameter. MOMENT is known to produce neutrinos by generating beams of μ^+ and μ^- , which are assumed to be produced in equal amounts in our baseline setup. This is one of the characteristics that can be changed in MOMENT. In Fig. 5, we show how $\Delta\delta_{\text{CP}}$ (1σ CL) changes for $\delta_{\text{CP}} = 0^\circ, 90^\circ, 180^\circ$ and 270° when the beam time is shared between the two polarities in asymmetrical running times. For this purpose, we define the quantity $\mu^+ / (\mu^+ + \mu^-)$ as the fraction at which MOMENT runs in μ^+ mode, whereas the rest of the 10-year-long running time is dedicated to μ^- mode.

The following observations can be made from Fig. 5: For the CP conserving values $\delta_{\text{CP}} = 0^\circ$ and 180° , we find a mild preference for the symmetrical running of 5+5 years. When $\delta_{\text{CP}} = 90^\circ$ or 270° , a pure μ^+ beam run is preferred instead, though it should be noted that the preference for the 10+0-year running time is not significant in the case of $\delta_{\text{CP}} = 90^\circ$.

We searched for the reason why the $\Delta\delta_{\text{CP}}$ distributions take different shapes for $\delta_{\text{CP}} = 0^\circ, 90^\circ, 180^\circ$ and 270° in Fig. 5. We find that the sensitivity to $\Delta\delta_{\text{CP}}$ is dominated by specific oscillation channels for different values of $\mu^+ / (\mu^+ + \mu^-)$. Whereas events from the $\nu_e \rightarrow \nu_\mu$ appearance channel constitutes the sensitivity when $\mu^+ / (\mu^+ + \mu^-)$ is close to one,

the sensitivity to δ_{CP} arises mainly from $\nu_\mu \rightarrow \nu_e$ events when the value of $\mu^+ / (\mu^+ + \mu^-)$ is close to zero. The impact of the corresponding antineutrino channels is negligible due to low signal-to-background ratio. For the true values $\delta_{\text{CP}} = 0^\circ$ and 180° , the effect of $\nu_e \rightarrow \nu_\mu$ and $\bar{\nu}_\mu \rightarrow \bar{\nu}_e$ channels is nearly symmetric, yielding nearly equal contributions to the $\Delta\delta_{\text{CP}}$ distribution. For the true values of $\delta_{\text{CP}} = 90^\circ$ and 270° , however, there exists a subtle asymmetry in favour of $\nu_e \rightarrow \nu_\mu$ events, giving $\Delta\delta_{\text{CP}}$ lower values for longer running times in the positive muon mode. While the preference is mild for $\delta_{\text{CP}} = 90^\circ$, the effect is noticeable when $\delta_{\text{CP}} = 270^\circ$.

We also investigated how changing the systematic uncertainties in the signal and background events as well as the detector coefficients and the size of the background changes the 1σ confidence level uncertainties in Fig. 5. We made the following remarks:

- Increasing the signal error σ_{sg} up to 15% leads to negligible changes in $\Delta\delta_{\text{CP}}$ when $\delta_{\text{CP}} = 90^\circ$ or 270° . For $\delta_{\text{CP}} = 0^\circ$ and 180° , however, $\Delta\delta_{\text{CP}}$ increased significantly.
- When the background error σ_{bg} was increased up to 15%, the change in $\Delta\delta_{\text{CP}}$ was less than 1° for all considered values of δ_{CP} .
- Changing the detector efficiencies lead to a shift in $\Delta\delta_{\text{CP}}$ distributions that has milder effect when the $\mu^+ / (\mu^+ + \mu^-)$ ratio is close to one. Conversely, the change in $\Delta\delta_{\text{CP}}$ is stronger when the ratio is close to zero. We observed similar effects for altering the size of the background.
- All of the changes in $\Delta\delta_{\text{CP}}$ conserved the shape mainly due to fact that the variations of experimental parameters were always imposed symmetrically on all of the oscillation channels. Were any of the neutrino appearance channels favoured over the others, the change might have also shown in the shapes.

We remark that the results presented in Fig. 5 were obtained when NO was assumed. We find the difference to be negligible when IO is considered.

4.2.4 First and second oscillation maxima

We also study the effect of the first and second oscillation maxima in the precision on δ_{CP} parameter. The first oscillation maximum occurs when the condition $\Delta L/2 \equiv L \Delta m_{31}^2 / 4E = \pi/2$ is met. For the proposed baseline length of MOMENT, $L \simeq 150$ km, the second oscillation maximum occurs for neutrino energies $E \simeq 300$ MeV. The second oscillation maximum follows similarly from the equation $\Delta L/2 = 3\pi/2$, which indicates $E \simeq 100$ MeV. We can therefore expect MOMENT to be sensitive to both the first and second oscillation maxima, with more events coming from the second maximum.

In theory, the experimental setup of MOMENT can be optimized to match the first oscillation maximum instead of the second one. In our simulation of MOMENT, the mean value of the neutrino energies is $E \simeq 200$ MeV. For these energies, the first oscillation maximum occurs at $L \simeq 50$ km and the second maximum at $L \simeq 150$ km. We therefore choose to compare the sensitivity to $\Delta\delta_{\text{CP}}$ at 1σ CL in MOMENT at baseline lengths 50 km

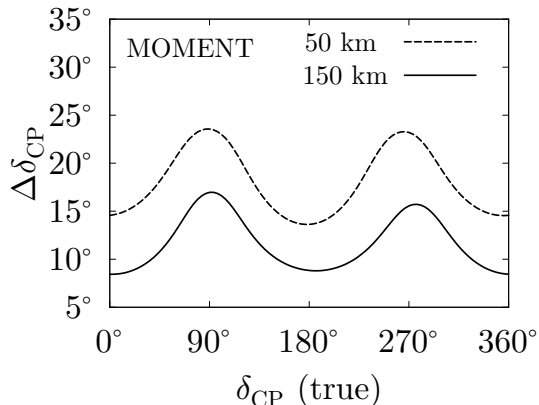


Figure 6: The effect of the first oscillation maximum on the precision measurement of δ_{CP} . The 1σ confidence level uncertainty of δ_{CP} is shown for two baseline lengths, $L = 50$ km and 150 km, which correspond to the experimental configurations where MOMENT is optimized for the first and second oscillation maximum, respectively. The results are independent of the mass ordering.

and 150 km. The results are shown for NO in Fig. 6. We find the results nearly identical when IO is considered.

In Fig. 6, the $\Delta\delta_{\text{CP}}$ distributions are shown in two scenarios. Whereas the solid line illustrates the $\Delta\delta_{\text{CP}}$ contour (1σ CL) as function of δ_{CP} values at 150 km baseline length, the dashed curve corresponds to the $\Delta\delta_{\text{CP}}$ contour at 50 km length with the same integrated luminosity. Whilst the first case corresponds to the baseline setup of MOMENT, the latter case corresponds to the situation where MOMENT is optimized for the first oscillation maximum. It is evident from the figure that the second oscillation maximum leads to a greater sensitivity on $\Delta\delta_{\text{CP}}$ for all available values of δ_{CP} . This is true despite the fact that at 50 km, the expected number of neutrino and antineutrino events at the far detector is expected to be nine times higher in comparison to the 150 km baseline length.

4.3 Complementarity of MOMENT and superbeam experiments in the measurement of δ_{CP}

In previous sections, we have investigated how well the parameter δ_{CP} can be measured in MOMENT, and how the sensitivities of MOMENT compare with those of the currently running and planned long baseline neutrino experiments. In this part of the work, we study how precisely the value of δ_{CP} can be determined after MOMENT finishes running.

The complementarity of the superbeam experiments and MOMENT play an important role in the determination of the δ_{CP} value at a high 1σ CL precision. Although MOMENT has access to a greater number of neutrino oscillation channels and lower beam backgrounds than superbeam experiments, the greater statistics provided by DUNE and T2HK near the first oscillation maximum improve the expected resolution on δ_{CP} throughout its currently allowed values. T2HKK can be expected to improve the precision further, as it provides

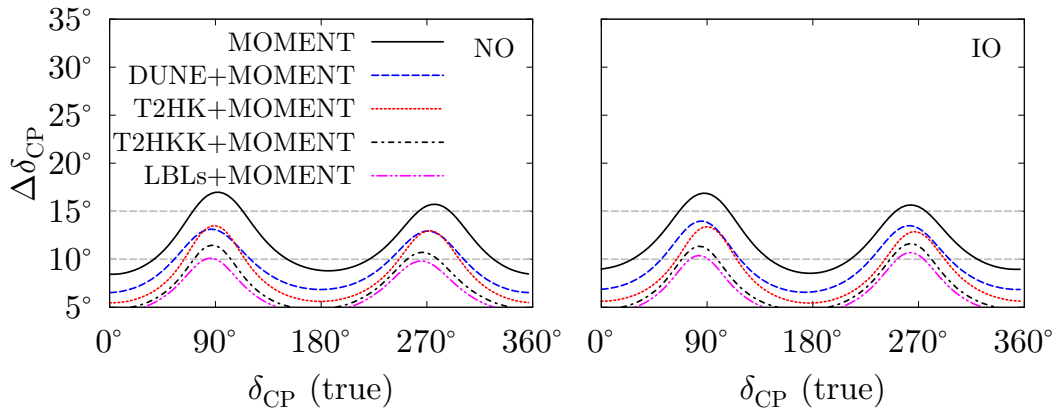


Figure 7: The 1σ confidence level uncertainty of δ_{CP} shown for four different combinations of neutrino oscillation data. The results are shown for the currently allowed values of δ_{CP} in normal ordering (NO) and inverted ordering (IO). The grey dashed lines represent the benchmark values of $\Delta\delta_{\text{CP}} = 10^\circ$ and 15° . Here LBLs+MOMENT corresponds to the combined run of the DUNE, MOMENT and T2HKK experiments.

events from both the first and second oscillation maximum [26]. The inclusion of the currently running experiments T2K and $\text{NO}\nu\text{A}$, however, can be expected to yield a non-significant contribution due to their relatively limited statistics.

In Fig. 7, we show the 1σ CL uncertainty of δ_{CP} as function of δ_{CP} values when the simulated data from MOMENT is analyzed jointly with that of either DUNE (dashed line), T2HK (dotted) or T2HKK (dot-dashed), and in the event when the data from MOMENT, DUNE and T2HKK are analyzed together (dot-dot-dashed). We also present the expected sensitivity to $\Delta\delta_{\text{CP}}$ at 1σ CL also for the event when only the data from MOMENT is analyzed. T2K and $\text{NO}\nu\text{A}$ are not included in the simulation. We have ascertained that their contribution is negligible.

Basing on the results shown in Fig. 7, we find that MOMENT has an appreciable sensitivity to measure the δ_{CP} parameter at 1σ CL. After 10 years of taking data, MOMENT can be expected to determine the value of δ_{CP} by greater than 20° resolution throughout the δ_{CP} value spectrum, and by 15° or better for 79% of the currently allowed values, regardless of the mass ordering. At the 10° discrimination level, we find MOMENT to be able to reach the desired resolution for 38% and 36% of the values in NO and IO, respectively.

The 1σ CL constraints on the true value of δ_{CP} can be improved further when the data from MOMENT is analyzed jointly with those of the currently planned long baseline experiments T2HK and DUNE. When the data from DUNE and MOMENT are analyzed together, we find the experiments to be able to measure the value of δ_{CP} by 10° or better at 1σ CL for 63% regardless of the mass ordering. When the data from DUNE is replaced with that of T2HK, on the other hand, the 10° coverage extends to 69% for both NO and IO. Replacing the data from T2HK with that of T2HKK instead improves the result to 82% in NO and 80% in IO, respectively. The most precise result can be expected from the

scenario where DUNE, MOMENT and T2HKK are able to conduct their planned runs, in which case the value of δ_{CP} can be determined at 1σ CL by at least 10° for 98% and 90% of the considered δ_{CP} values for NO and IO, respectively.

In our concluding remark, we briefly comment on the prospects of measuring the value of δ_{CP} in the next-generation accelerator experiments when the true value of δ_{CP} is 270° . When the neutrino masses are normally ordered, we find MOMENT to be able to determine the value of δ_{CP} by 15.6° at 1σ CL, whereas the inclusion of either the DUNE or T2HK data could improve the precision to 12.9° , and of T2HKK to 10.7° , respectively. Combining the data from MOMENT, DUNE and T2HKK could yield an overall resolution of 10.1° , and 9.3° when MOMENT is let to run entirely in μ^+ mode. All results are obtained at 1σ CL. We obtained similar results for the inverted mass ordering.

5 Summary

We have investigated the physics reach of MOMENT in the measurement of Dirac CP phase δ_{CP} , and compared its sensitivities to those of the planned superbeam experiments T2HK, T2HKK and DUNE, as well as the running T2K and NO ν A. With the proposed setup [17], we find the sensitivities in MOMENT to be comparable with those of T2HK and T2HKK and greater than the sensitivities simulated in DUNE, T2K and NO ν A.

We have studied the effect of several experimental characteristics on the precision measurement of δ_{CP} , in order to identify potential bottlenecks and opportunities for improvement in MOMENT. We have investigated the effect of statistical and systematic uncertainties, changing the fraction of the positive/negative beam polarity in the total running time, and adjusting the baseline length to match the first or second oscillation maximum on the precision measurement of δ_{CP} . Our results are summarized in Table 3.

The current design of MOMENT provides the advantage of delivering a low-background beam where the systematic uncertainties can be assumed to be relatively low. This in turn gives the experiment a leverage on measuring the value of δ_{CP} near the CP conserving values of $\delta_{\text{CP}} = 0^\circ$ and 180° . An exception to this feature is seen near the maximally CP violating values of $\delta_{\text{CP}} = 90^\circ$ and 270° , where systematics only play a small role and improvements to the CP precision must be achieved by increasing the statistics.

The CP precision in MOMENT has been previously studied in Refs. [18] and [19], where the simulated neutrino and antineutrino fluxes peak between 100...200 MeV. In the present work, the results are presented for a configuration where the beam is optimized for the second oscillation maximum. The beam fluxes described in this paper are also used in Refs. [20] and [21]. We find that this setup leads to a greater resolution on δ_{CP} .

Altogether, we find that MOMENT has an excellent potential to constrain the δ_{CP} parameter value to about 10° or better at 1σ confidence level, when its data is analyzed together with those of the proposed superbeam experiments T2HKK and DUNE. The same resolution can also be achieved in MOMENT alone by increasing its statistics by a factor of four.

We conclude this work with the following remarks:

Table 3: The impact of statistical error, systematic uncertainties, changing the fraction of the positive/negative beam polarity in the total running time and adjusting the beam energy and baseline setup to match the first and second oscillation maximum on $\Delta\delta_{\text{CP}}$ for $\delta_{\text{CP}} = 0^\circ, 90^\circ, 180^\circ$ and 270° at 1σ confidence level. The values are shown for the normal mass ordering. The final column shows references to the relevant figures.

δ_{CP}	0°	90°	180°	270°	Figure
Running times					Fig. 3
10 years	8.4°	17.0°	8.2°	15.6°	
40 years	5.2°	8.9°	5.6°	8.0°	
Systematics					Fig. 4
2%	8.2°	16.9°	8.6°	15.5°	
15%	15.1°	17.5°	18.1°	16.0°	
Beam polarity					Fig. 5
50%/50%	8.4°	17.0°	8.8°	15.6°	
100%/0%	10.3°	16.6°	11.0°	12.8°	
Oscillation maximum					Fig. 6
1 st max.	14.6°	23.6°	13.6°	23.2°	
2 nd max.	8.4°	17.0°	8.8°	15.6°	

- Our simulation shows excellent precision in the measurement of δ_{CP} in MOMENT. With the proposed setup, the sensitivities in MOMENT are comparable with those of T2HKK and T2HK and greater than those DUNE.
- For the current best-fit values, MOMENT can reach the approximate precision of 10.0° at 1σ confidence level in normal ordering and 14.3° in inverted ordering, respectively.
- Many of the experimental parameters in MOMENT are still open for discussion. We have found that in the case of $\delta_{\text{CP}} = 270^\circ$, the highest precision on δ_{CP} can be obtained when the experiment runs entirely in the μ^+ mode.
- MOMENT can improve the δ_{CP} bounds from those of T2HK and DUNE significantly. When the three are analysed together, we find that MOMENT can improve δ_{CP} precision to 11.8° or better at 1σ confidence level, regardless of the mass ordering or the true value of δ_{CP} . When T2HKK is considered instead of T2HK, the precision improves to 10.7° , respectively.

Acknowledgments

This work is supported in part by the National Natural Science Foundation of China under Grant Nos. 11505301 and 11881240247, and by the university support based on National SuperComputer Center-Guangzhou (74130-31143408). We would like to thank the accelerator working group of MOMENT for providing the neutrino flux files. We also thank Dr. Nick W. Prouse for the T2HKK simulation package.

6 Appendix

A The long baseline neutrino experiments considered in this work

In this appendix, we list the long baseline experiments that have been considered in this work. We also describe how the simulation of each experiment was created.

A.1 T2K

The Tokai-to-Kamioka (T2K) [22] experiment is a currently running long-baseline neutrino oscillation experiment in Japan with a 295 km baseline. The neutrino and antineutrino beams of predominantly muon flavour are generated via pion decay in the J-PARC facility in Tokai, where a 30 GeV proton beam is directed at a graphite target. The neutrino beam and subsequently the antineutrino beam are first studied at the near detectors ND280 and INGRID, which are both located approximately 280 meters from the target. The far detector facility in Kamioka is Super-Kamiokande, which is a Water Čerenkov detector of 22.5 kton of fiducial mass located at 2.5° off-axis from the beam. The produced neutrino and antineutrino beams peak at roughly 600 MeV, which corresponds to the first oscillation maximum for $\nu_\mu \rightarrow \nu_e$ and $\bar{\nu}_\mu \rightarrow \bar{\nu}_e$ channels. T2K began operating in 2011, and it is expected to yield a total of 7.8×10^{21} protons-on-target (POT) with 2 years of neutrino run and 6 years of antineutrino run.

In our simulation of T2K, we assume a full 2+6-year running time in neutrino and antineutrino modes, 22.5 kton of fiducial mass and 0.77 MW beam power. The studied energy range is 0.4 GeV...1.2 GeV, which is divided into 20 energy bins of equal size. The energy resolution is taken to be a constant 0.085 GeV to account the Fermi motion. For more details regarding the simulation, see the GLOBES website [40].

A.2 NO ν A

The NuMI Off-axis ν_e Appearance (NO ν A) [23] is another on-going long baseline neutrino oscillation experiment, which is currently operating in the United States. NO ν A consists of the NuMI beam facility and a near detector in Fermilab, and of a 14 kt Liquid Scintillator detector located in Ash River, Minnesota. The far detector is located 810 km from the source at 14.6 mrad off-axis, where the first oscillation maximum occurs for $\nu_\mu \rightarrow \nu_e$ and $\bar{\nu}_\mu \rightarrow \bar{\nu}_e$ approximately at 2 GeV. The near detector on the other hand, consists of 200 ton and it is located 1 km from the source along the axis. Both the near and far detectors are highly active tracking calorimeters segmented with hundreds of PVP cells. NO ν A began

running in 2014 and it is expected to reach the exposure of 3.6×10^{21} POT after running 3 years in neutrino mode and 3 years in antineutrino mode.

In our simulation of $\text{NO}\nu\text{A}$, we adopt the simulation files that are available on the GLOBES website [40]. We changed the fiducial mass of the detector and the expected POT number to 14 kton and 3.6×10^{21} , respectively.

A.3 T2HK and T2HKK

The Tokai-to-Hyper-Kamiokande (T2HK) experiment [24] is a next-generation neutrino oscillation experiment and a successor to T2K. T2HK will use a beam setup similar to its predecessor T2K, that is, a 2.5 degree off-axis beam from J-PARC. Before T2HK starts operating, the beam facility will be upgraded to 1.3 MW power and Hyper-Kamiokande [42] will take over Super-Kamiokande as the far detector. The new detector will consist of two Water Čerenkov tanks, equivalent to 187 kton fiducial mass each. The experiment is expected to run 2.5 years in neutrino mode and 7.5 years in antineutrino mode, expecting a total exposure of 1.56×10^{22} POT. An alternative of placing the second detector in Korea instead has also been considered under the T2HKK proposal [26].

In this work, we conduct the simulation for T2HK and T2HKK using simulation files that were provided by the T2HK collaboration. In the case of T2HK, we assume a staged approach where the experiment runs the first six years with one detector and the other four years with two detectors. Both detector vessels are taken to be located at 295 km from the source. For the simulation of T2HKK, on the other hand, we assume a full 10-year run with the second detector vessel placed in Korea at 1100 km from the source, whilst the first detector vessel is located in Kamioka at 295 km. For the Korea detector, we assume a 1.5° off-axis angle.

A.4 DUNE

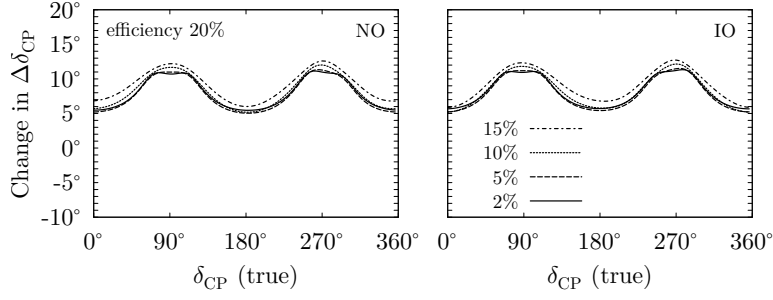
The Deep Underground Neutrino Experiment (DUNE) [25, 43–45] is a next generation long-baseline neutrino experiment currently under construction in the United States. Its design features the LBNF neutrino beam in Fermilab and a 40 kton far detector located in the Sanford Underground Research Facility at the Homestake mine, located 1300 km from the source. The detector is based on the Liquid Argon Time Projection Chamber technology. The beam consists of muon neutrinos and antineutrinos peaking roughly at 2.5 GeV energy. A total exposure of 1.47×10^{21} POT is expected for DUNE after running 3.5 years in neutrino mode and 3.5 years in antineutrino mode. A multipurpose near detector is located approximately at 500 m from the source. DUNE is expected to begin its run in 2026.

In our simulation of DUNE, we adopt the simulation files that were provided by the DUNE collaboration, see Ref. [41] for more details.

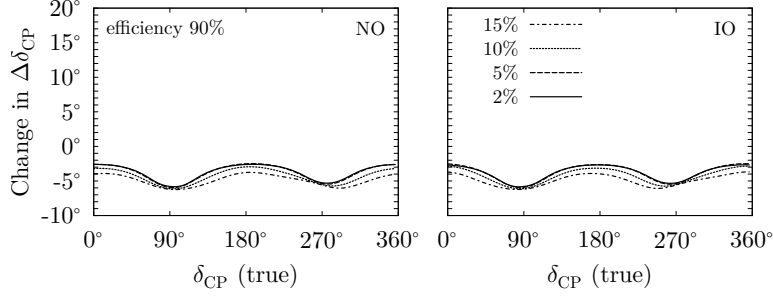
B The effects of detector efficiencies and atmospheric neutrino background on the results

In this appendix, we provide more details on how different assumptions on the systematic uncertainties, detector efficiencies and background size affect the $\Delta\delta_{\text{CP}}$ distributions we obtained for MOMENT. This discussion is necessary, as many of the technical details of MOMENT are still uncertain. Among the unsettled questions are at least the performance of the Gd-doped Water Čerenkov technology and the suppression of the atmospheric neutrino background.

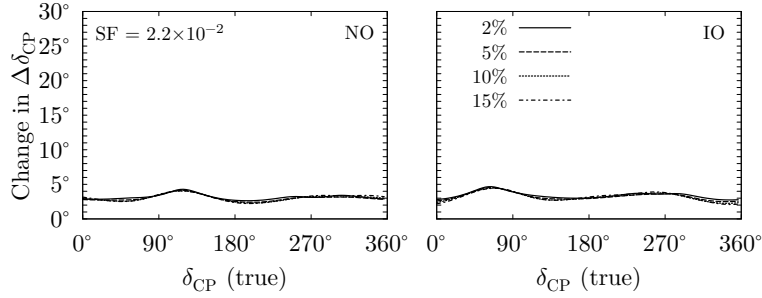
In Fig. 8, we present the deviations that occur in $\Delta\delta_{\text{CP}}$ distributions when the systematic uncertainties of the experiment are varied under different assumptions on the detector efficiencies and the atmospheric neutrino background. In panels 8a and 8b, the change in $\Delta\delta_{\text{CP}}$ is calculated when the detector efficiencies in signal channels are set to 20% and 90%, respectively. Panels 8c and 8d on the other hand represent the situations where the suppression factor for the atmospheric neutrino background is taken to be 2.2×10^{-2} and 2.2×10^{-1} . Both results are compared to that of the baseline setup, where the suppression factor is assumed to be 2.2×10^{-3} . The atmospheric neutrino background and the suppression factor are defined in Eq. (3.1) in Section 3.



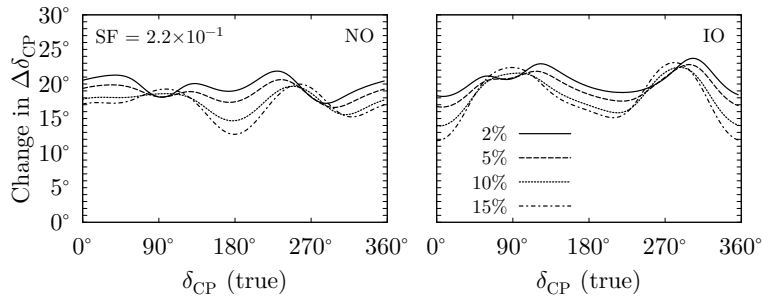
(a) Detector efficiencies 20%



(b) Detector efficiencies 90%



(c) Suppression factor 2.2×10^{-2}



(d) Suppression factor 2.2×10^{-1}

Figure 8: The effect of detector efficiencies and atmospheric neutrino background on $\Delta\delta_{\text{CP}}$ in MOMENT when the signal errors are set to 2%, 5%, 10% or 15%. Deviations from the results obtained with the baseline setup are presented for $\Delta\delta_{\text{CP}}$ when detector efficiencies are set to (a) 20% or (b) 90%, and when the atmospheric neutrino background is suppressed by a factor of (c) 2.2×10^{-2} and (d) 2.2×10^{-1} instead of 2.2×10^{-3} , respectively. The atmospheric neutrino background is calculated with Eq. (3.1). The results are shown for both normal ordering (NO) and inverted ordering (IO).

References

- [1] T. Kajita and Y. Totsuka, *Observation of atmospheric neutrinos*, *Rev. Mod. Phys.* **73** (2001) 85.
- [2] SNO collaboration, *Measurement of the rate of $\nu_e + d \rightarrow p + p + e^-$ interactions produced by 8B solar neutrinos at the Sudbury Neutrino Observatory*, *Phys. Rev. Lett.* **87** (2001) 071301 [[nucl-ex/0106015](#)].
- [3] B. Pontecorvo, *Mesonium and anti-mesonium*, *Sov. Phys. JETP* **6** (1957) 429.
- [4] Z. Maki, M. Nakagawa, Y. Ohnuki and S. Sakata, *A unified model for elementary particles*, *Prog. Theor. Phys.* **23** (1960) 1174.
- [5] M. Kobayashi and T. Maskawa, *CP Violation in the Renormalizable Theory of Weak Interaction*, *Prog. Theor. Phys.* **49** (1973) 652.
- [6] “NuFIT 4.1 (2019).” <http://www.nu-fit.org/>.
- [7] I. Esteban, M. C. Gonzalez-Garcia, A. Hernandez-Cabezudo, M. Maltoni and T. Schwetz, *Global analysis of three-flavour neutrino oscillations: synergies and tensions in the determination of θ_{23} , δ_{CP} , and the mass ordering*, *JHEP* **01** (2019) 106 [[1811.05487](#)].
- [8] P. F. De Salas, S. Gariazzo, O. Mena, C. A. Ternes and M. Tortola, *Neutrino Mass Ordering from Oscillations and Beyond: 2018 Status and Future Prospects*, *Front. Astron. Space Sci.* **5** (2018) 36 [[1806.11051](#)].
- [9] F. Capozzi, E. Lisi, A. Marrone and A. Palazzo, *Current unknowns in the three neutrino framework*, *Prog. Part. Nucl. Phys.* **102** (2018) 48 [[arXiv:1804.09678](#)].
- [10] S. F. King, *Models of Neutrino Mass, Mixing and CP Violation*, *J. Phys.* **G42** (2015) 123001 [[1510.02091](#)].
- [11] S. T. Petcov and A. V. Titov, *Assessing the Viability of A_4 , S_4 and A_5 Flavour Symmetries for Description of Neutrino Mixing*, *Phys. Rev.* **D97** (2018) 115045 [[1804.00182](#)].
- [12] P. Ballett, S. F. King, S. Pascoli, N. W. Prouse and T. Wang, *Sensitivities and synergies of DUNE and T2HK*, *Phys. Rev.* **D96** (2017) 033003 [[1612.07275](#)].
- [13] M. Ghosh and T. Ohlsson, *A comparative study between ESSnuSB and T2HK in determining the leptonic CP phase*, [1906.05779](#).
- [14] P. Coloma, A. Donini, E. Fernandez-Martinez and P. Hernandez, *Precision on leptonic mixing parameters at future neutrino oscillation experiments*, *JHEP* **06** (2012) 073 [[1203.5651](#)].
- [15] W. Winter, *Understanding CP phase dependent measurements at neutrino superbeams in terms of bi-rate graphs*, *Phys. Rev.* **D70** (2004) 033006 [[hep-ph/0310307](#)].
- [16] M. V. Smirnov, Z. J. Hu, S. J. Li and J. J. Ling, *The possibility of leptonic CP-violation measurement with JUNO*, *Nucl. Phys.* **B931** (2018) 437 [[1802.03677](#)].
- [17] J. Cao et al., *Muon-decay medium-baseline neutrino beam facility*, *Phys. Rev. ST Accel. Beams* **17** (2014) 090101 [[1401.8125](#)].
- [18] M. Blennow, P. Coloma and E. Fernández-Martinez, *The MOMENT to search for CP violation*, *JHEP* **03** (2016) 197 [[1511.02859](#)].
- [19] P. Bakhti and Y. Farzan, *CP-Violation and Non-Standard Interactions at the MOMENT*, *JHEP* **07** (2016) 109 [[1602.07099](#)].

- [20] J. Tang and Y. Zhang, *Study of nonstandard charged-current interactions at the MOMENT experiment*, *Phys. Rev.* **D97** (2018) 035018 [[1705.09500](#)].
- [21] J. Tang, T.-C. Wang and Y. Zhang, *Invisible neutrino decays at the MOMENT experiment*, *JHEP* **04** (2019) 004 [[1811.05623](#)].
- [22] T2K collaboration, *The T2K Experiment*, *Nucl. Instrum. Meth.* **A659** (2011) 106 [[arXiv:1106.1238](#)].
- [23] NOvA collaboration, *The NOvA Technical Design Report*, *FERMILAB-DESIGN-2007-01* (2007) .
- [24] HYPER-KAMIOKANDE PROTO-COLLABORATION collaboration, *Physics potential of a long-baseline neutrino oscillation experiment using a J-PARC neutrino beam and Hyper-Kamiokande*, *PTEP* **2015** (2015) 053C02 [[arXiv:1502.05199](#)].
- [25] DUNE collaboration, *Long-Baseline Neutrino Facility (LBNF) and Deep Underground Neutrino Experiment (DUNE)*, [arXiv:1512.06148](#).
- [26] HYPER-KAMIOKANDE collaboration, *Physics potentials with the second Hyper-Kamiokande detector in Korea*, *PTEP* **2018** (2018) 063C01 [[1611.06118](#)].
- [27] K. Asano and H. Minakata, *Large-Theta(13) Perturbation Theory of Neutrino Oscillation for Long-Baseline Experiments*, *JHEP* **06** (2011) 022 [[1103.4387](#)].
- [28] P. Huber, M. Lindner and W. Winter, *Simulation of long-baseline neutrino oscillation experiments with GLOBES (General Long Baseline Experiment Simulator)*, *Comput. Phys. Commun.* **167** (2005) 195 [[hep-ph/0407333](#)].
- [29] P. Huber, J. Kopp, M. Lindner, M. Rolinec and W. Winter, *New features in the simulation of neutrino oscillation experiments with GLOBES 3.0: General Long Baseline Experiment Simulator*, *Comput. Phys. Commun.* **177** (2007) 432 [[hep-ph/0701187](#)].
- [30] MEMPHYS collaboration, *Study of the performance of a large scale water-Cherenkov detector (MEMPHYS)*, *JCAP* **1301** (2013) 024 [[1206.6665](#)].
- [31] J. F. Beacom and M. R. Vagins, *GADZOOKS! Anti-neutrino spectroscopy with large water Cherenkov detectors*, *Phys. Rev. Lett.* **93** (2004) 171101 [[hep-ph/0309300](#)].
- [32] J.-E. Campagne, M. Maltoni, M. Mezzetto and T. Schwetz, *Physics potential of the CERN-MEMPHYS neutrino oscillation project*, *JHEP* **04** (2007) 003 [[hep-ph/0603172](#)].
- [33] E. Fernandez-Martinez, *The gamma = 100 beta-Beam revisited*, *Nucl. Phys.* **B833** (2010) 96 [[0912.3804](#)].
- [34] E. A. Paschos and J. Y. Yu, *Neutrino interactions in oscillation experiments*, *Phys. Rev.* **D65** (2002) 033002 [[hep-ph/0107261](#)].
- [35] P. Huber, M. Lindner and W. Winter, *Superbeams versus neutrino factories*, *Nucl. Phys.* **B645** (2002) 3 [[hep-ph/0204352](#)].
- [36] Y. Itow et al., *The jhf-kamioka neutrino project*, [hep-ex/0106019](#).
- [37] M. Ishitsuka, T. Kajita, H. Minakata and H. Nunokawa, *Resolving neutrino mass hierarchy and cp degeneracy by two identical detectors with different baselines*, *Phys. Rev.* **D72** (2005) 033003 [[hep-ph/0504026](#)].
- [38] NOvA collaboration, *Nova proposal to build a 30-kiloton off-axis detector to study neutrino oscillations in the fermilab numi beamline*, [hep-ex/0503053](#).

- [39] NOVA collaboration, *Study of physics sensitivity of ν_μ disappearance in a totally active version of nova detector*, [Off-Axis-Note-SIM-30](#).
- [40] “GLOBES (2018).” <https://www.mpi-hd.mpg.de/personalhomes/globes/>.
- [41] DUNE collaboration, *Experiment Simulation Configurations Used in DUNE CDR*, [arXiv:1606.09550](#).
- [42] HYPER-KAMIOKANDE collaboration, *Hyper-Kamiokande Design Report*, .
- [43] DUNE collaboration, *Long-Baseline Neutrino Facility (LBNF) and Deep Underground Neutrino Experiment (DUNE)*, [1601.05471](#).
- [44] DUNE collaboration, *Long-Baseline Neutrino Facility (LBNF) and Deep Underground Neutrino Experiment (DUNE)*, [1601.05823](#).
- [45] DUNE collaboration, *Long-Baseline Neutrino Facility (LBNF) and Deep Underground Neutrino Experiment (DUNE)*, [1601.02984](#).